Thermochimica Acta, 199 (1992) 133–146
Elsevier Science Publishers B.V., Amsterdam

Thermal analysis of thermoplastic matrices for advanced composite materials: poly(phenylene sulphide) [1]

A. Maffezzoli, J.M. Kenny and L. Nicolais

Dipartimento di Ingegneria dei Materiali e della Produzione, Università di Napoli Federico II, P. le Tecchio, 80125 Naples (Italy)

(Received in final form 26 September 1991)

Abstract

Evolution of the thermal and viscoelastic properties of a poly(phenylene sulphide) (PPS) neat resin and a PPS–matrix composite during crystallization from the amorphous state at low temperatures (cold crystallization) and from the molten state at higher temperatures (melt crystallization) has been investigated by differential scanning calorimetry (DSC) and dynamic mechanical analysis (DMA). The degree of crystallization is correlated to the experimental signal measured by both techniques. Two relations between the viscoelastic properties (storage modulus and storage compliance) and the volume fraction of crystallinity are analysed on the assumption of in-parallel and in-series connections of two generic viscoelastic elements, representing the amorphous and crystalline phases. A clearer picture emerges from the in-series hypothesis.

INTRODUCTION

In recent years, the growing commercial importance of the high-performance thermoplastic polymers adopted as matrices for structural composites has promoted intensive research on the characterization of their morphological and mechanical properties. Semicrystalline matrices, such as poly(ether ether ketone) (PEEK), poly(phenylene sulphide) (PPS), and thermoplastic polyimide (TPI), in particular offer high temperature service and good environmental resistance, and are being used as matrices of carbon fibre composites for some aircraft component applications.

Compared to thermoset based composites, thermoplastic matrices present advantages in terms of processability. Processing of semicrystalline matrices displays particular features due to the presence and evolution of the crystalline phase. Semicrystalline polymers heated above the glass transition temperature T_g, or cooled below the melting temperature T_m,

Correspondence to: J.M. Kenny, Dipartimento di Ingegneria dei Materiali e della Produzione, Università di Napoli Federico II, P. le Tecchio, 80125 Napoli, Italy.

[1] Presented at the 12th National Conference on Calorimetry and Thermal Analysis, Bari, Italy, 11–13 December 1990.

can crystallize at a rate controlled by the crystallization temperature. During normal processing, the polymer matrix is first heated above T_m. The material is then formed by applying the appropriate technology (thermoforming, pultrusion, filament winding, etc.) and cooled to room temperature. Imposition of different thermal conditions strongly affects the crystallinity content and morphology of the formed parts, and consequently their mechanical properties and environmental and chemical resistance [1–4]. For these reasons, study of the crystallization behaviour of PPS-based composites is particularly interesting.

During crystallization, melting or annealing experiments, the dynamic mechanical properties of semicrystalline polymers, as well as their thermal and dielectric properties, undergo marked changes owing to evolution of the crystalline phase [4,5]. Calorimetry has already been used to investigate crystallization of the PPS polymer and PPS–matrix composites [6–10], but there is little information on their viscoelastic properties [11,12].

In this paper, the evolution of the thermal and viscoelastic properties during crystallization of PPS neat resin and PPS–matrix composites is presented. Crystallizations from the amorphous state at low temperatures (cold crystallization), and from the molten state at higher temperatures (melt crystallization), are examined by differential scanning calorimetry (DSC) and dynamic mechanical analysis (DMA). Furthermore, different approaches to analysis of the dynamic mechanical data and correlation of the DMA and DSC results are proposed.

EXPERIMENTAL

The experiments were performed on a PPS prepreg, Ryton AC-66 (fibre content 60%; thickness 0.16 mm) reinforced with carbon fibre, and a neat PPS film (thickness 0.8 mm). The material was kindly provided by Phillips Petroleum Co. The calorimetric analysis was carried out with a Mettler DSC 30 differential scanning calorimeter (DSC) operating from −50 to +450°C in a nitrogen atmosphere. Test samples were approximately 30–40 mg prepreg or 10–20 mg neat resin. DSC analysis of the as-received materials confirmed that they can be considered fully amorphous. The dynamic mechanical properties of the samples were evaluated with a Du Pont 983 dynamic mechanical analyser (DMA). The experiments were carried out in the forced oscillation mode at a frequency of 2 Hz on single-ply composite samples.

CALORIMETRIC ANALYSIS

The properties and applications of PPS place it between two well known semicrystalline polymers, PEEK widely used for high-performance composites, and PET used for low and medium technology applications. Typical

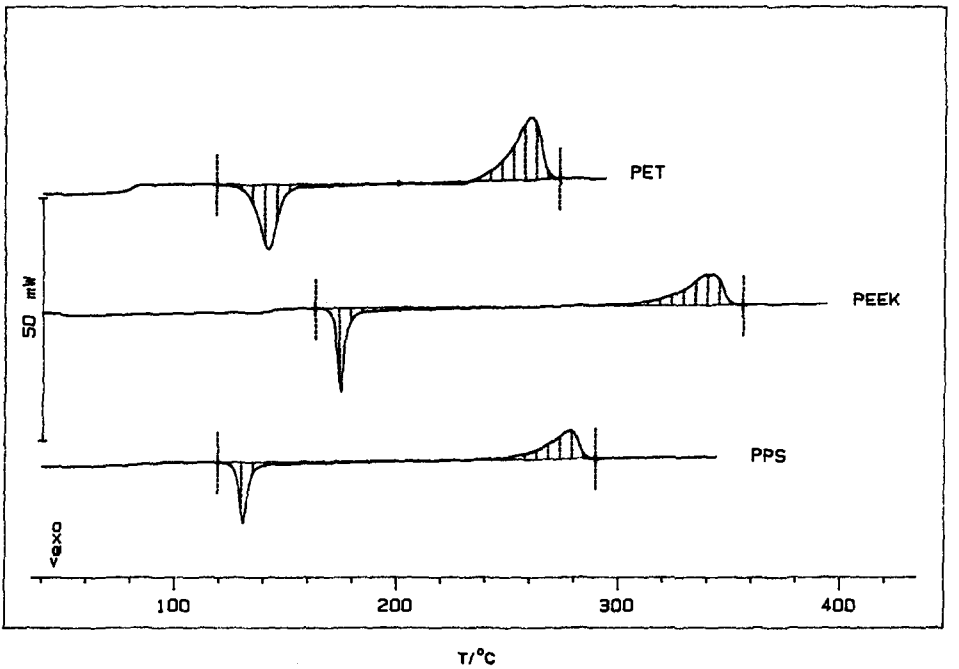

Fig. 1. DSC thermograms obtained at 10°C min^{-1} on three initially amorphous polymers.

dynamic DSC scans (10°C min^{-1}) of the three initially amorphous polymers (Fig. 1) show three main anomalies, the glass transition ($T_g = 85$°C for PPS), a sharp exothermal crystallization peak above T_g, and an endothermal melting peak ($T_m = 274$°C for PPS).

Cold and melt crystallization processes can be studied by heating amorphous samples over the glass transition temperature, or by rapidly cooling them from the melt to the test temperature respectively. Two typical isothermal DSC cold and melt crystallization thermograms are reproduced in Fig. 2. The delay in the DSC signal is an induction phenomenon associated with crystallite nucleation. A relationship between the DSC signal and the degree of crystallization must be assumed to enable calorimetric data to be used in the study of crystallization kinetics. The proportionality between the rate of crystallization and the heat flow measured by DSC, reported in the literature [1,2,9], leads to a simple expression for calculation of the mass fraction of crystallinity (X_{mc})

$$X_{mc} = 1/Q_f \int_0^t dQ/dt \; dt \tag{1}$$

where Q_f is the heat of fusion of the pure crystal and dQ/dt is the measured heat flow starting from the baseline as shown in Fig. 2.

The results of the low-temperature isothermal tests are compared in Table 1. The negligible differences between the maximum degree of

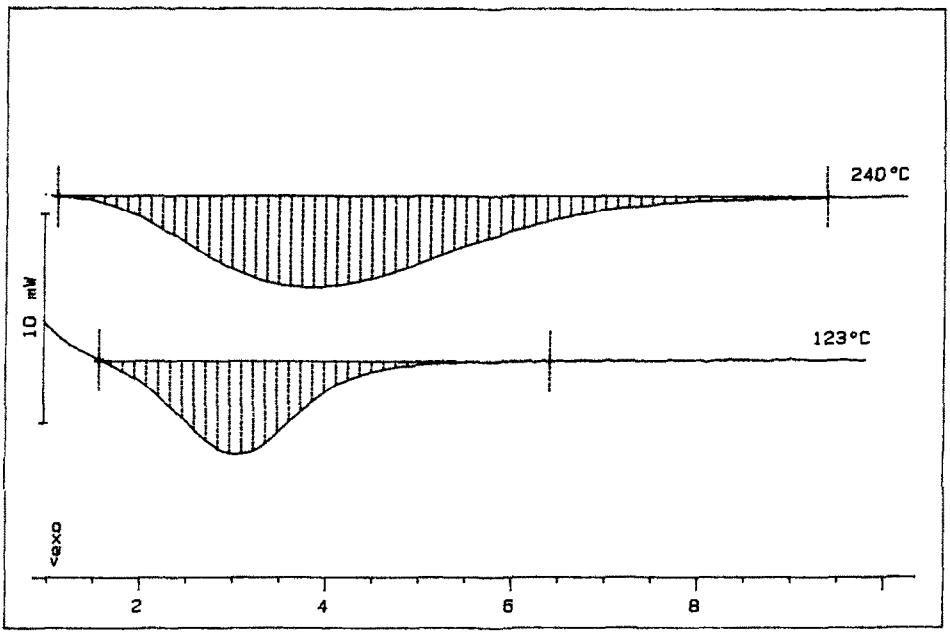

Fig. 2. DSC isothermal thermograms obtained during the cold and melt crystallization of the neat resin.

crystallization (X_{vcmax}) values for the two materials suggest that fibres have no substantial effect on the total amount of PPS crystallinity in cold crystallization. Furthermore, while the induction times (t_i) for the two

TABLE 1

DSC characterization of cold crystallization

T (°C)	t_i (s)	t_c (s)	n	X_{vcmax}	X_{vcs}
Composite					
125	78	474	1.75	0.29	
127	63	264	1.72	0.30	
130	60	240	1.81	0.26	
132	50	230	1.7	0.26	
135	50	218	1.55	0.23	
Neat resin					
120	84	372	2.27	0.26	0.23
123	93	222	2.16	0.26	0.23
125	78	108	2.37	0.27	0.26
127	80	88	2.29	0.27	0.22
130	70	82	2.09	0.27	0.23
132	57	84	2.1	0.26	0.20
135	46	104	1.91	0.25	0.17

TABLE 2

DSC characterization of melt crystallization

T (°C)	t_i (s)	t_c (s)	X_{vcmax}	n
Composite				
230	47	616	0.40	1.91
232	49	826	0.45	2.08
235	63	954	0.43	2.02
240	87	1263	0.43	1.97
Neat resin				
230	47	364	0.50	1.84
232	55	538	0.55	2.19
235	57	576	0.54	2.14
240	98	785	0.50	2.12
245	54	1350	0.51	2.08

materials are of the same order, the composite is characterized by longer crystallization times (t_c), suggesting that fibres retard the growth process.

The values of X_{vcmax} of the neat resin are higher during melt crystallization (Table 2). This effect of carbon fibres has also been reported for PEEK [3] and can be attributed to restriction of the volume available for the crystal growth. Once again, t_c times are higher for the composite, while the t_i times are similar. The different behaviour observed between cold and melt crystallization with respect to X_{vcmax} can also be interpreted in terms of geometrical restriction of the fibres to the crystal growth. At low temperatures, low levels of crystallinity are due to the limited mobility of the amorphous phase; hence the restraining effect of the fibres is negligible. In melt crystallization, higher crystallinity levels are reached and the effect of the fibres on crystal growth is enhanced.

The crystallization behaviour of PPS can be better understood through an Avrami analysis of the data, using the expression

$$X_{vcr} = 1 - \exp(-kt^n) \tag{2}$$

where $X_{vcr} = X_{vc}/X_{vcmax}$ is the relative volume fraction of crystallinity, X_{vc} is the volume fraction of crystallinity, t is the crystallization time, n is the Avrami exponent and k is a temperature-dependent rate constant. The exponent n is characteristic of the geometry of crystal nucleation and growth, and can be calculated from the experimental data by rearranging eqn. (2).

$$\ln[-\ln(1 - X_{vcr})] = \ln k + n \ln t \tag{3}$$

Plots of the cold and melt crystallization data and the theoretical results predicted by eqn. (3) are drawn in Fig. 3 for both materials. The Avrami exponents calculated by linear regression are included in Tables 1 and 2.

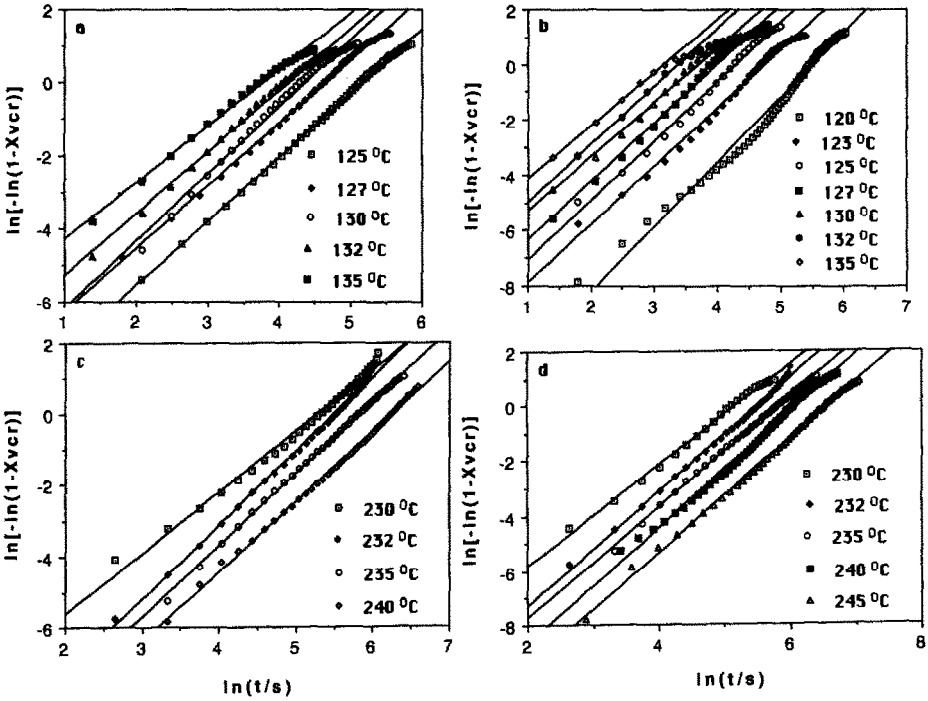

Fig. 3. Avrami plot from calorimetric data: (a) cold crystallization of the composite; (b) cold crystallization of the neat resin; (c) melt crystallization of the composite; (d) melt crystallization of the neat resin.

The slope of the Avrami plots for cold crystallization of the neat resin (Fig. 3(b)) shows a roll-off after a significant fraction of crystallinity is developed (X_{vcs} in Table 1). This effect, also reported for PEEK [2], can be attributed to secondary growth due to restriction of crystal growth induced by the limited mobility of the amorphous phase at low temperatures. The same behaviour is less evident for the composite (Fig. 3(a)) probably because of the small quantity of heat involved in this secondary growth process. A single slope behaviour is displayed by both materials in melt crystallization (Fig. 3(c) and 3(d)). This result substantiates the effect of molecular mobility on the crystal growth. The value of n is always of the order of 2, suggesting that cold and melt crystallization of both materials occur through bidirectional growth of a circular lamellar geometry.

An Arrhenius expression is adopted for the temperature dependence of the rate constant k (eqn. (2)) for the two crystallization processes

$$k = k_0 \exp(-E_a/RT) \tag{4}$$

where E_a is an activation energy associated with the crystallization process and k_0 is a pre-exponential constant. Values of E_a have been calculated by linear regression of values of ln k obtained as a function of $1/T$ (Table 3).

TABLE 3

Parameter values used in eqn. (4)

Parameter	Composite	Neat resin
Cold crystallization		
E_a (kJ mol^{-1})	424	545.5
ln k_0 (s^{-1})	119	155
Melt crystallization		
E_a (kJ mol^{-1})	−354.3	−515.5
ln k_0 (s^{-1})	−95.6	−133.7

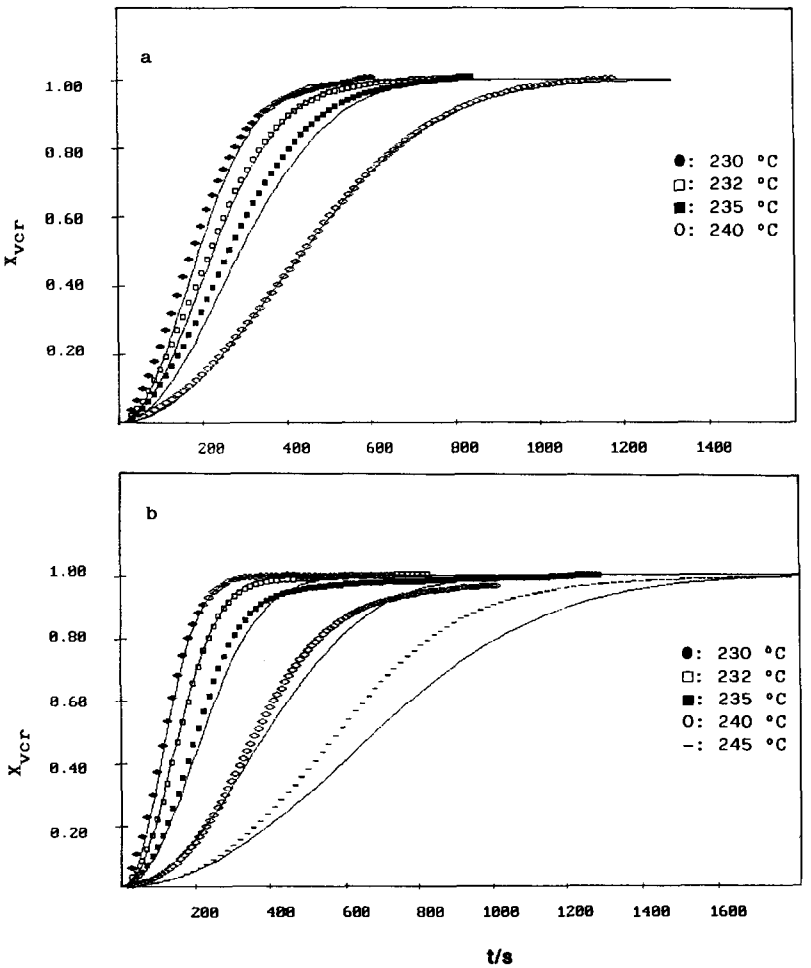

Fig. 4. Comparison between experimental data and theoretical prediction of eqns. (2) and (4) for melt crystallization: (a) composite; (b) neat resin.

The very high E_a values obtained indicate strong dependence of the crystallization kinetics on the process temperature. Equation (4) gives a good approximation of the temperature dependence of k only in the range explored. Crystallization rates, in fact, reach a maximum between T_g and T_m: for cold crystallization, occurring below this maximum, the activation energy will be positive, whereas it is negative for melt crystallization, occurring above this maximum.

The crystallization model given by eqns. (2) and (4) has been tested by comparing the melt crystallization data and the theoretical predictions. The parameter values in Table 3 were adopted with average values $n = 2$ and $n = 2.1$. The close fit between the experimental data and the theoretical predictions in Fig. 4(a) (composite) and Fig. 4(b) (neat resin) confirms the ability of the model to represent crystallization in this temperature range. The irregular behaviour of the Avrami plots makes a similar comparison impossible for cold crystallization.

DYNAMIC MECHANICAL ANALYSIS

The results of DMA tests (3°C min^{-1}) on three samples with different initial crystallinity are shown in Fig. 5. The drop of the storage modulus (E') in the glass transition region is dramatically evident for the initially

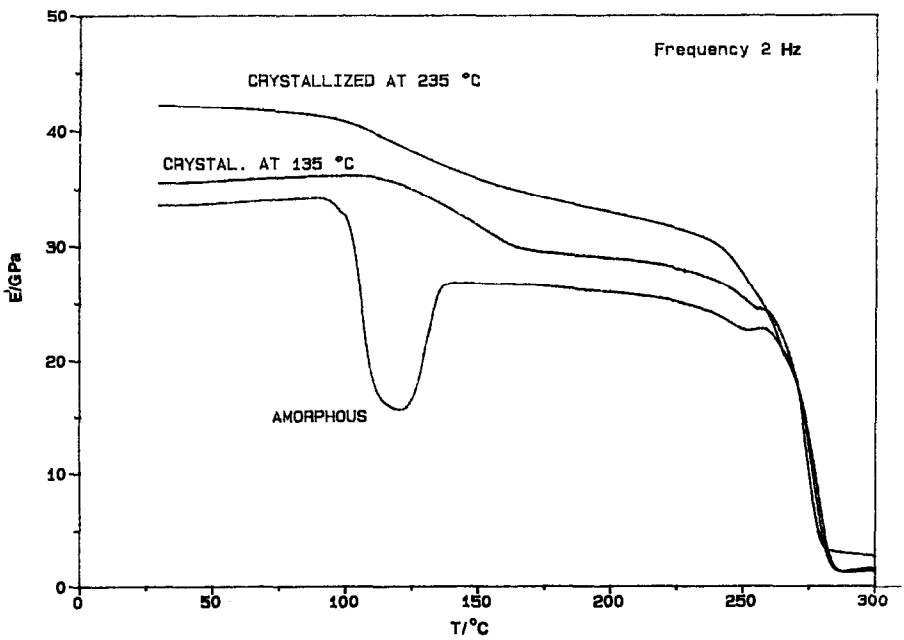

Fig. 5. Storage modulus as a function of the temperature (3°C min^{-1}) for three samples with a different initial crystallinity.

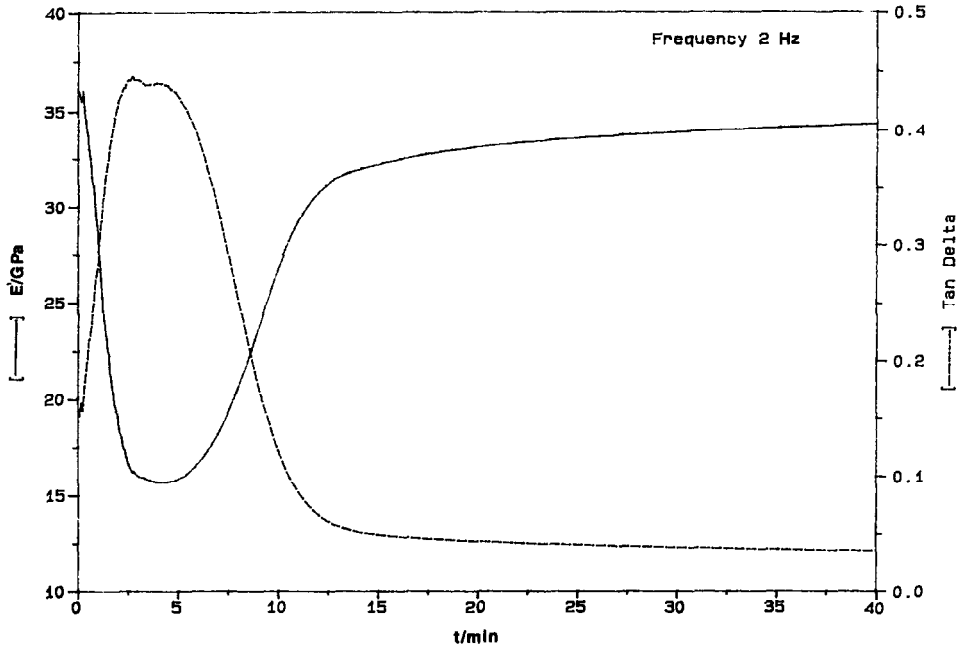

Fig. 6. DMA results of isothermal cold crystallization at 125°C on the composite.

amorphous sample. Above T_g the amorphous PPS is in the rubbery state and the crystallization is activated by increased molecular mobility. The crystalline phase acts as a reinforcing agent and is responsible for the subsequent increase of the modulus. As the melting region is approached, the storage moduli of the three samples fall to very small values. The sample crystallized from the melt shows a higher modulus than that crystallized from the amorphous state. This effect is due to their different maximum degrees of crystallization, and confirms the DSC results in Tables 1 and 2.

Typical cold crystallization DMA results obtained during an isothermal test (125°C) on the "as-received" amorphous matrix composite are shown in Fig. 6. The evolution of E' and the loss factor (tan delta) clearly reflects the effect of the reinforcing crystalline phase on the viscoelastic properties. Moreover, the initial decrease of E' is probably due to the effect of the nucleation time, also detected in DSC experiments. However, the results in the first part of the experiment may be affected by an inevitable initial gap between the recorded temperature and the sample temperature. This effect, in fact, is related to higher thermal loads involved in DMA tests, and is not detected in the DSC experiments with shorter response times. Therefore, it has been assumed that the onset of crystallization is represented by the E' minimum. This assumption implies higher indetermination of the DMA technique compared to DSC for crystallization kinetic analysis, mainly during the first stages of the test.

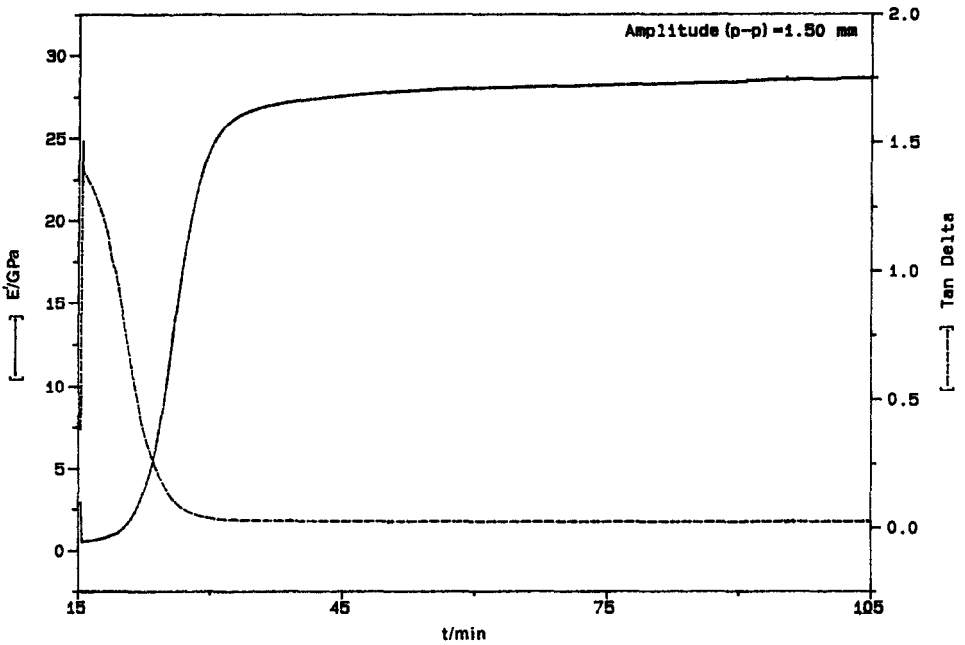

Fig. 7. DMA results of isothermal melt crystallization at 240°C on the composite.

A similar behaviour is obtained in the isothermal melt crystallization of the composite reported in Fig. 7. Here, too, it has been assumed that the starting point of the crystallization is represented by the minimum of the E' curve.

During the isothermal crystallization experiments illustrated in Figs. 6 and 7, the composite experiences strong changes in its viscoelastic properties owing to transition from a fully amorphous rubbery state to a semicrystalline morphology with both a crystalline and an amorphous rubbery phase. To study crystallization, the evolution of a viscoelastic property measured by DMA must be related to the phenomena occurring in the sample. Assuming that the viscoelastic behaviour of the crystalline and the amorphous phases can be represented by two generic viscoelastic elements, a parallel connection between them can be hypothesized, and the relation between the complex moduli can be derived [13]

$$E^* = (1 - X_{vc})E_a^* + X_{vc}E_c^* \tag{5}$$

where E^*, E_a^* and E_c^* are, respectively, the complex moduli of the composite, and the amorphous and crystalline phases. By combining the real and imaginary terms in eqn. (5), similar expressions for E' and loss modulus (E'') can be easily derived

$$E' = (1 - X_{vc})E_a' + X_{vc}E_c' \tag{6}$$

$$E'' = (1 - X_{vc})E_a'' + X_{vc}E_c'' \tag{7}$$

Rearrangement of eqn. (7) gives the following expression for X_{vcr}, as reported for the analysis of PEEK crystallization [1,5,14]

$$X_{vcr} = (E' - E'_0)/(E'_{max} - E'_0) \tag{8}$$

where E'_0 is the modulus of the fully amorphous material at the crystallization temperature and E'_{max} is the maximum modulus reached in an isothermal experiment.

Assumption of in-series connection of two viscoelastic elements representing the amorphous and crystalline phases, however, leads to a linear relationship between the complex compliances

$$S^* = (1 - X_{vc})S_a^* + X_{vc}S_c^* \tag{9}$$

where S^* is the complex compliance of the composite, and S_a^* and S_c^* are the complex compliances of the amorphous and crystalline phases respectively. An expression analogous to eqn. (8) can again be developed

$$X_{vcr} = (S' - S'_0)/(S'_{max} - S'_0) \tag{10}$$

In eqn. (10), S' is the measured storage compliance, S'_0 is the storage compliance of the fully amorphous material at the crystallization temperature, and S'_{max} is the maximum storage compliance reached during the isothermal experiment.

The in-parallel connection between the two viscoelastic elements gives a linear relationship between E' and X_{vcr} (eqn. (8)). The in-series connection leads to a linear relationship between S' and X_{vcr} (eqn. (10)). Moreover, a combination of parallel and series connections between the two phases can also be defined [13]. While only one simple relationship has been assumed between the DSC data and the degree of crystallization, many different hypotheses and relationships can be formulated for the correlation of the DMA data and the degree of crystallization.

An Avrami analysis of the cold crystallization DMA data for PPS composite has been performed by assuming a parallel connection, using eqns. (2) and (6). The results obtained for four crystallization temperatures are reported in Fig. 8. As in DSC, two main slopes, reflecting two kinetic processes, characterize the DMA curves. This behaviour has been reported in calorimetric studies of other semicrystalline matrices [2] and can be attributed to two different crystal growth processes, the second one representing a secondary growth due to the restrictions imposed by low matrix mobility, the effect of the fibres, and impingement of different crystallizing fronts. X_{vcr} values at the break point in the slope (X_{vcrb}) calculated from the calorimetric model (eqns. (2) and (4)) are reported in Table 4. A significant fraction of the modulus has been developed before the second kinetic process starts. X_{vcrb} values close to unity indicate that only a limited additional crystallization is responsible for a marked additional increase in the viscoelastic properties after the break point. This additional

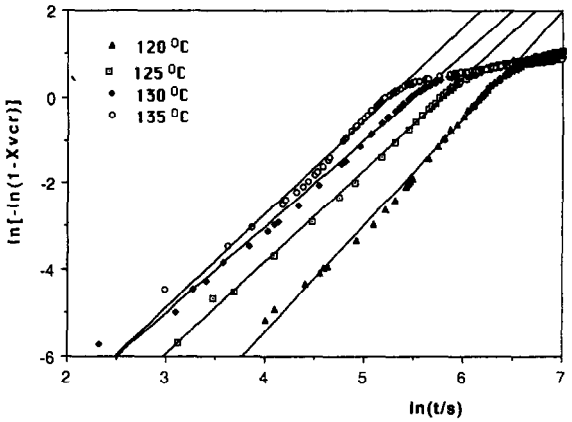

Fig. 8. Avrami plot obtained for the cold crystallization of the composite by calculating the relative volume fraction of crystallinity from dynamic storage moduli (eqn. (8)).

crystallization (the second slope in Fig. 8) probably represents a morphological change in the crystalline structure, responsible for a marked increase in the modulus, rather than the degree of crystallization. The two DMA slopes are thus less evident on the Avrami plots of the calorimetric data (Fig. 3(a)). Furthermore, there is a good fit between the Avrami exponents calculated from the first slopes in Fig. 8 (Table 4) and those in Table 1.

The dynamic storage moduli for melt crystallization of the PPS–matrix composite have also been transformed by applying the in-parallel connection hypothesis between the crystalline and amorphous phases (eqns. (2) and (6)). An Avrami plot of these results (lower curve of Fig. 9) for an isothermal test is characterized by a two-slope curve, representative of the main crystallization, while, at long times, a straight line can be associated with a secondary crystallization process. However, the DSC data (Fig. 3(b)) show a single slope for the main crystallization process.

TABLE 4

DMA results: cold and melt crystallization

Cold crystallization			Melt crystallization		
T (°C)	X_{vcrb}	n	T (°C)	X_{vcrb}	n
120	0.90	2.4	228	0.98	1.9
123	0.90	2.0	232	0.98	1.5
125	0.95	2.1	235	0.94	1.7
127	0.98	2.2	240	0.70	1.7
130	0.99	2.0	245	0.83	1.5
135	0.99	2.2			

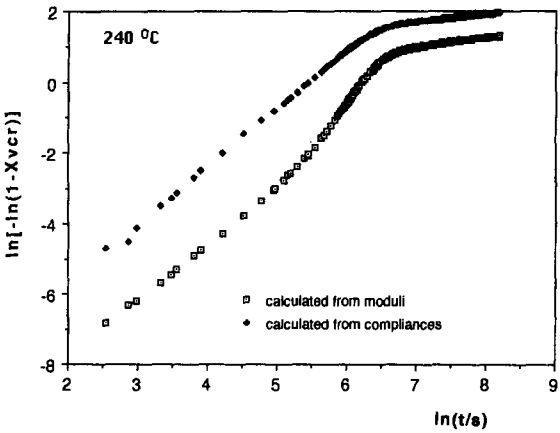

Fig. 9. Comparison of two Avrami plots obtained for the melt crystallization of the composite by calculating the relative volume fraction of crystallinity by dynamic storage moduli (eqn. (8)) and by dynamic storage compliances (eqn. (9)).

The upper curve in Fig. 9 represents the transformation according to the in-series connection hypothesis (eqn. (10)). The definite two-straight-line behaviour, similar to that for cold crystallization, again indicates a double kinetic mechanism. Furthermore, a better agreement between the DSC and the DMA results is obtained. The corresponding Avrami plots, obtained using eqns. (2) and (10), are reported in Fig. 10. The Avrami exponents for the first kinetic mechanism (Table 4) agree with those in Table 2. The X_{vcrb} values are also close to unity. However, the flatness of the second slope indicates little additional increase in the viscoelastic properties, suggesting

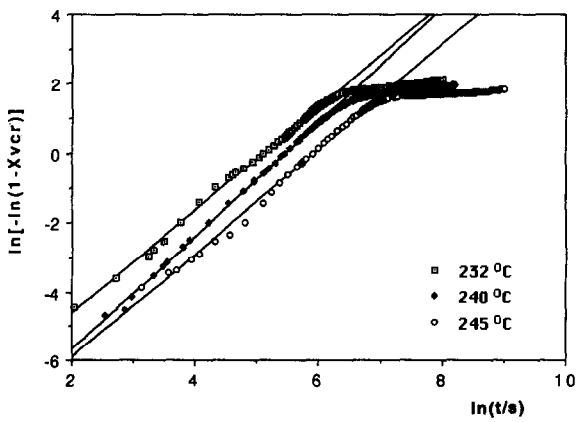

Fig. 10. Avrami plot obtained for the melt crystallization of the composite by calculating the relative volume fraction of crystallinity from dynamic storage compliances (eqn. (10)) at three temperatures.

that most of the morphological crystalline structure is developed during the first process.

CONCLUSIONS

Different types of information were obtained when DSC and DMA were used to investigate the cold and melt crystallization of PPS as neat polymer and as a matrix of carbon fibre composites. DSC gave a clearer picture of the correlation between the degree of crystallization and the measured data. It also allowed easier detection of the rapid changes in the degree of crystallization at the beginning of the tests thanks to a shorter response time due to the smaller sample size. However, the changes occurring in the last part of the crystallization experiments were more evident from the DMA data. Lastly, two relations between the viscoelastic properties (storage modulus and storage compliance) and the volume fraction of crystallinity were applied to study crystallization of the PPS–matrix composite. The DMA results present a clearer picture when the degree of crystallization is correlated to the changes in dynamic storage compliance of a system with two generic viscoelastic elements representing the amorphous and crystalline phases of the polymer connected in series.

ACKNOWLEDGEMENT

The financial support of Alenia Saipa is gratefully acknowledged.

REFERENCES

1 J.M. Kenny, A. D'Amore, L. Nicolais, M. Iannone and B. Scatteia, SAMPE J., 25 (1989) 27.
2 P. Cebe and S.D. Hong, Polymer, 27 (1986) 1183.
3 C.N. Velisaris and J.C. Seferis, Polym. Eng. Sci., 26 (1986) 1574.
4 A. Maffezzoli, J.M. Kenny, L. Torre and L. Nicolais, Proc. 11th Int. SAMPE Symp., Eur. Chapt., Basel, Switzerland, May 1990, p. 307.
5 A. D'Amore, J.M. Kenny, L. Nicolais and V. Tucci, Polym. Eng. Sci., 30 (1990) 314.
6 D.J. Brady, J. Appl. Polym. Sci., 20 (1976) 2541.
7 L.C. Lopez and G.L. Wilkes, Polymer, 29 (1988) 106.
8 G.P. Jog and V.M. Nadkarni, J. Appl. Polym. Sci., 30 (1985) 997.
9 J.M. Kenny and A. Maffezzoli, Polym. Eng. Sci., 31 (1991) 607.
10 P. Cebe and S. Chung, Polym. Compos., 11 (1990) 265.
11 C.M. Ma, H. Hsia, W. Liu and J. Hu, Polym. Compos., 8 (1987) 256.
12 A. Maffezzoli, J.M. Kenny and L. Nicolais, Proc. 49th SPE ANTEC, Montreal, Canada, May 1991, p. 2079.
13 M. Takayanagi, K. Imada and T. Kajiyama, J. Polym. Sci., Part C, 15 (1966) 263.
14 A. Kitano and J.C. Seferis, Proc. 35th Int. SAMPE Symp., Anaheim, USA, April 1990, p. 2260.